Journal of Basic and Applied Engineering Research
Print ISSN: 2350-0077; Online ISSN: 2350-0255; Volume 1, Number 2; October, 2014 pp. 57-64

http://www.krishisanskriti.org/jbaer.html

Advanced Approaches in Superplastic Forming-A Case Study

R. J. Bhatt

S V National Institute of Technology, Surat, Gujarat, India

Abstract: **Superplasticity is the term used to indicate the exceptional ductility that certain metals can exhibit when deformed under specific conditions of strain rate and temperature, such property found in titanium, aluminium, magnesium and nickel alloys. Superplastic forming (SPF) has become most viable in manufacturing aircraft, automobile and commercial parts as turbine blades, window frames, seat structures, honeycomb structures etc. Superplastic forming involves the shaping of metal sheets by gas pressure at elevated temperatures. It relies on the fact that fine-grained metals can exhibit high sensitivities of flow stresses to strain rate, but this usually only occurs at quite slow strain rates. As a result, the process is much slower than conventional pressing operations and the major factor is the process cost. So that SPF has been mostly limited to low-volume production due to relatively long cycle times that can exceed 30 minutes.**

This study incorporates the advanced approaches employed to SPF process. Moreover, case studies i) hybrid superplastic forming with hot draw mechanical pre-forming and ii) design and validation of two stage superplastic forming are also being reported. The first novel process involves hot drawing with SPF process that utilizes mechanical pre-forming to enhance formability, reduce costs and improve production efficiency. The second advanced process is used for reduction of thinning. In this process within a single die, gas pressure is used to form the blank into a preform die cavity prior to the pressure being reversed to form the sheet into the final component cavity. The pre-forming of the blank creates length of line, while preserving metal thickness in certain regions to improve the thickness profile of the final part. These processes eliminate the limitations like slow forming rate, material cost, excessive thinning etc.

1. INTRODUCTION

Superplastic forming technology exceeds the limit of standard press working technology in the form of thickness distribution. The conventional light weight alloys such as Aluminum, Magnesium and Titanium has limited formability due to their poor low temperature ductility so these materials can be formed very easily by means of SPF process. Among the light weight alloys these three received more attention due to their excellent physical and mechanical properties such as low density, high specific strength and specific rigidity, strong electromagnetic shielding, good thermal conductivity etc.

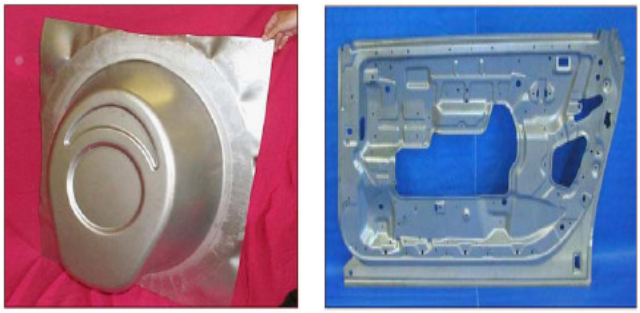

(a) **(b)**

Fig. 1: Typical applications of superplastic forming (a) Aerospace Component (b) Automotive door panel [1]

Blow forming and vacuum forming are conventional superplastic forming process. A gas pressure differential is imposed on the superplastic diaphragm, causing the material to form into the die configuration as shown in Fig. 2. In vacuum forming, the applied pressure is limited to atmospheric pressure (that is, 100 kPa, or 15 psi), and the forming rate and capability are therefore limited. With blow forming, additional pressure is applied from a gas pressure reservoir, and the only limitations are related to the pressure rating of the system and the pressure of the gas source.

A maximum pressure of 690 to 3400 kPa (100 to 500 psi) is typically used in this process. In this process, the dies and sheet material are normally maintained at the forming temperature, and the gas pressure is imposed over the sheet, causing the sheet to form into the lower die; the gas within the lower die chamber is simply vented to atmosphere. The lower die chamber can also be held under vacuum, or a back pressure can be imposed to suppress cavitations if necessary. Sometimes use a moving or adjustable die member in conjunction with gas pressure or vacuum.

Apart from this, there are several other superplastic forming techniques; such are Thermoforming, Deep Drawing, and Superplastic Forming/Diffusion Bonding etc.

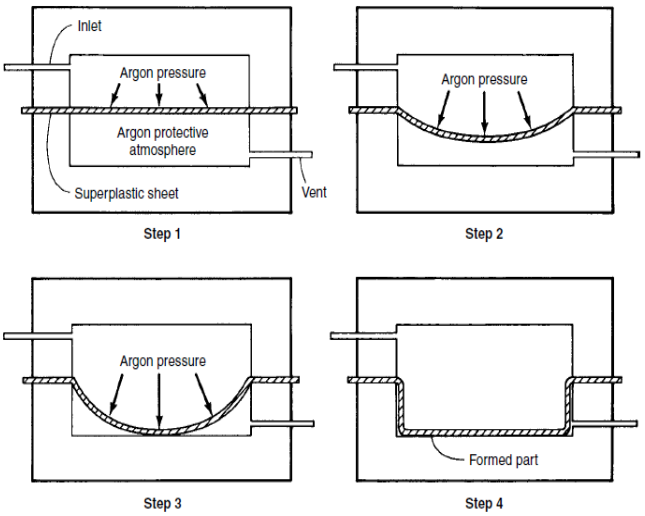

Fig. 2: Schematic of blow forming technique for Superplastic forming [2]

1.1 Advantages & Limitations of SPF

Advantages:

- Ability of forming complex parts in single operation with close tolerance
- Lower strength is required and less tooling cost
- Weight and material saving
- Little or no residual stress occurs in formed parts
- No spring back

Limitations

- Low productivity due to low strain rates
- Higher Material cost
- Longer cycle times

2. HYBRID SUPERPLASTIC FORMING WITH HOT DRAW MECHANICAL PRE-FORMING-CASE STUDY I

In this case, a novel SPF process is discussed that incorporates hot drawing with SPF. With the use of a blank holder during the drawing process, wrinkling can be suppressed while material is drawn into the die cavity. The drawing of metal into the die cavity prior to SPF offers several advantages. First, the final part is significantly thicker than a part made solely by SPF due to the additional metal in the forming cavity. Second, only a minimal amount of SPF is needed to complete the part so that optimized superplastic response in the material is not needed. This allows for very fast forming and the use of an alloy that is not specially processed for SPF. These advantages significantly affect total processing cost. The fact that the final part is thicker allows for down-gauging of the incoming sheet to reach the final part gauge, hence savings in material costs. The faster forming time translates to lower burden costs on the equipment.

2.1 Hot Draw Mechanical Pre-Forming Process

To address the limitations of SPF for medium- and high volume automotive manufacturing, such as the inability to draw material into the die cavity, a novel multi-stage SPF process was invented by combining hot stamping with SPF. This integrated process significantly reduces the cycle time by eliminating a large portion of the gas forming portion of the process while retaining the advantages of increased formability and zero springback.

This process contains two separate forming steps as noted in Fig. 3. The blank is first preheated external to the press within a proprietary automated preheater to the target forming temperature. After preheating, the blank is automatically loaded into the press. The sheet is initially loaded onto the heated blankholder, which is supported by a movable cushion system, as shown in Fig. 3 (a). The upper die is then lowered until it engages the blankholder and wraps the material around the punch. Once the blankholder reaches the die shoe Fig. 3 (b), the press tonnage is increased to seal the die. Gas is then introduced into the lower cavity to complete the part, as shown in Fig. 3 (c). After the part is completed, the gas pressure is released and the upper die is raised so that the completed part can be removed from the die.

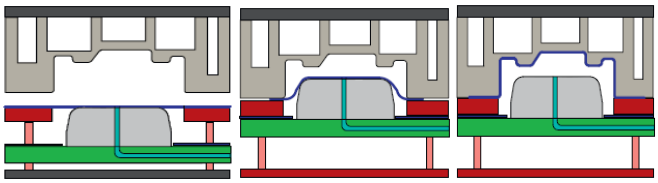

(a) (b) (c)

Fig. 3: Schematic of Hot draw mechanical pre-forming SPF process (a) the sheet is first loaded into the die set (b) a drawing stage pre-forms the sheet (c) a gas forming stage completes the forming operation [12]

2.2 Experimental Setup for HDMP SPF Process

To conduct the experiment three different materials have been chosen. First a specially processed fine-grain superplastic SPF5083 alloy was used in most of the forming trials and the only alloy used in the correlation of FEA results to experimental forming trials. SPF5083 alloy is currently the alloy of choice for automotive SPF applications because of its moderate strength, good corrosion resistance, relatively low cost and ease of processing to achieve a fine-grain structure. The sheet had a nominal thickness of 1.6 mm and was received in the fully hard (H19) condition. After annealing, the grain size was approximately 8 μm. Chemical composition of the alloy is listed in Table 1.

Table 1 Chemical Composition (wt%) of test SPF5083 (AA5083) alloy [12]

Material	Mg	Mn	Fe	Si	Cr	Cu
SPF5083	4.8	0.53	0.23	0.08	0.08	0.07

Ti	Al
0.03	rest

2.3 Constitutive model of SPF5083

To apply finite element analysis constitutive equation of material is required for thickness, material draw in and pressure cycle predictions. Flow stress for superplastic materials can be obtained by defining a viscoplastic potential and by assuming von Mises behavior for perfect viscoplasticity. A power-law equation of both strain and strain rate has been applied as the material model for the HDMP of the SPF5083 alloy. An FEA-based constitutive coefficient refinement method developed by Raman [8] that establishes an accurate stress, strain rate and strain relationship using high-temperature constant crosshead speed tensile test data was used to establish the constitutive coefficients.

Two sets of co-efficients have been set for HDMP and SPF process because the strain rate is faster in HDMP compared to gas forming process. Tensile test have been conducted for strain rate $4x10^{-4}$-10^{-1} s^{-1} and formulate constitutive model of SPF5083 for draw stage as given below:

$$\sigma = 75.32\ \dot{\varepsilon}^{-0.26}\varepsilon^{0.084} \quad (1)$$

For the gas forming lower strain rate $5x10^{-4}$ and $3x10^{-3}$ s^{-1} used with creep model coefficients.

$$\sigma = 159.5\ \dot{\varepsilon}^{-0.39}\varepsilon^{0.088} \quad (2)$$

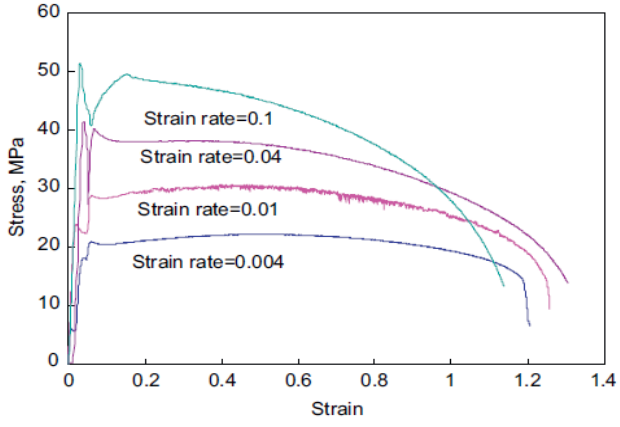

Fig. 4: True stress and true strain of SPF5083as determined by tensile test for different initial strain rates at 475 C. Rapid increase in flow stress at approximately 5% strain is due to intended jump in strain rate [12]

2.4 Simulation model

The three dimensional explicit finite element code LS-DYNA used to simulate the process. A simple square die was used for this initial study. Due to symmetry, a quarter section of the tool was modeled to minimize computation time. The sheet was constructed using shell elements, the punch and die were modeled as analytical rigid surfaces while the blankholder was modeled as an elastic body. The initial dimensions of the blank were 750mm x 750mm with a thickness of 1.6 mm. During the simulation, the lower die was fixed and the SPF5083 blank was held between blankholder and lower die, and drawn by the punch to the appropriate depth. The material is assumed to be isotropic due to the high forming temperature. It was assumed that the tooling was in an isothermal steady-state condition and thermal gradients were not considered in FEA simulation as the die temperature was maintained within ± 3 C of the target temperature during forming.

Simulation parameters: Friction at tool/sheet μ = 0.10, punch velocity = 8 mm/s, element size = 5 mm.

2.5 Experimental model

A HDMP-SPF die of square cavity was used in all forming trials. The upper die cavity had a length and a width of 400 mm, 20mm entry radii, 20mm corner radii and a depth of 150 mm. Risers of 25, 50 and 75mm in height were used to set the draw depth of the punch between 25 and 150 mm. The punch pre-form surface was offset from the forming cavity by at least 5mm to ensure the die set was not matching and to facilitate part removal. The radii of the pre-form were made as large as possible to reduce localized thinning in the sheet.

All forming trials were performed in an 800 ton hydraulic SPF press. Blanks were sheared to 750mm x 750mm from the same lot of material for each alloy. An alcohol wipe was used to remove the mill oil from each blank. The blanks were coated on both sides with a specially formulated lubricant that contains boron nitride. The die was secured to the press platens that contain cartridge heaters, which heat the platen and SPF die.

The experiments were performed at two conditions: HDMP-SPF and Gas only SPF. An optimized gas pressure cycle determined by FEA was applied to form the sheet.

2.6 Forming trials with SPF5083

All SPF5083 blanks were completely formed into the die cavity using the HDMP process, where the blanks were first mechanically pre-formed by drawing and then gas formed at a target strain rate of 5x10-3 s-1. The gas pressure forming cycle applied is shown in Fig. 5. Here overall forming of part was conducted 180 s, including 130 s of gas forming. Gas pressure profile as shown in Fig. 6 was used during only gas forming

with targeted strain rate of 10^{-3} s^{-1}. Examples of both HDMP-SPF and conventional SPF are shown in Fig 7.

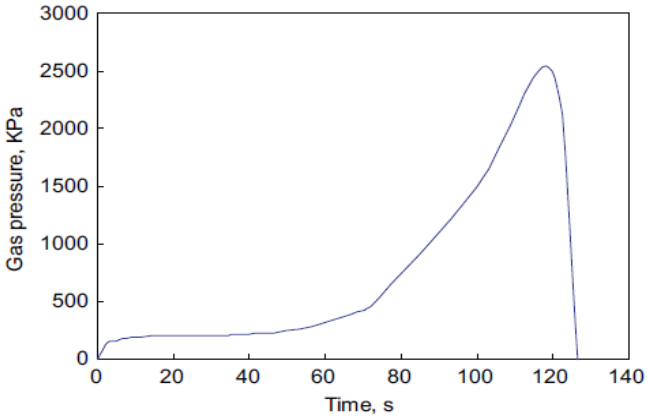

Fig. 5: Gas pressure cycle predicted by FEA for forming the rectangular die with SPF5083 at a target strain rate of 5x10-3 s-1 after pre-forming [12]

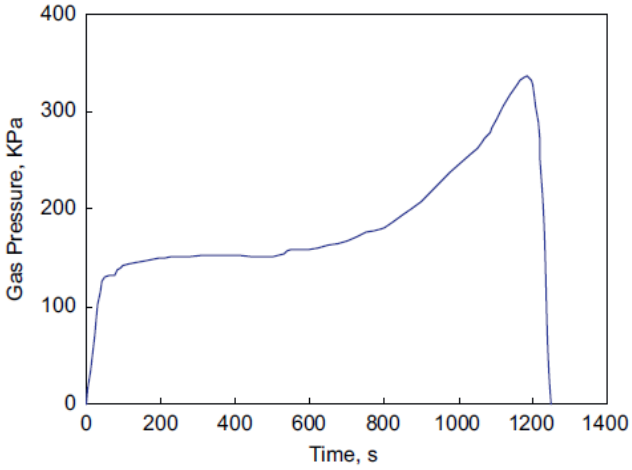

Fig. 6: Gas pressure cycle predicted by LS-DYNA for forming the rectangular die with SPF5083 at a target strain rate of 10-3 s-1 with gas forming only [12]

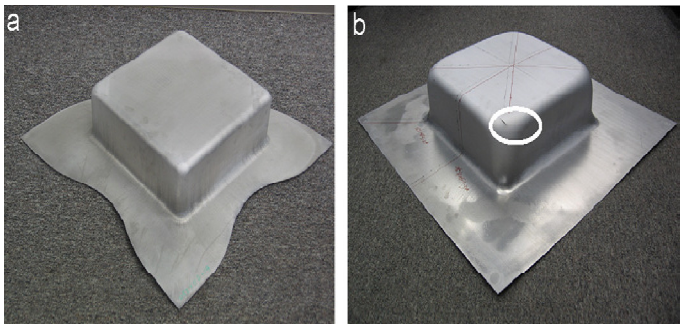

Fig. 7: Formed part of SPF5083 using (a) HDMP-SPF and (b) gas forming only [12]

Material draw-in was calculated by measuring the distance at the locations identified in Fig. 8. The line L0 is the width of the initial blank, L1 is the width of the part at the edge and line L2 is the span between middle points of the flange. The significant material was drawn into the die, especially at the middle of the blank. Additionally, the simulation result of material draw-in correlates well to the experimental results showing high predictive accuracy.

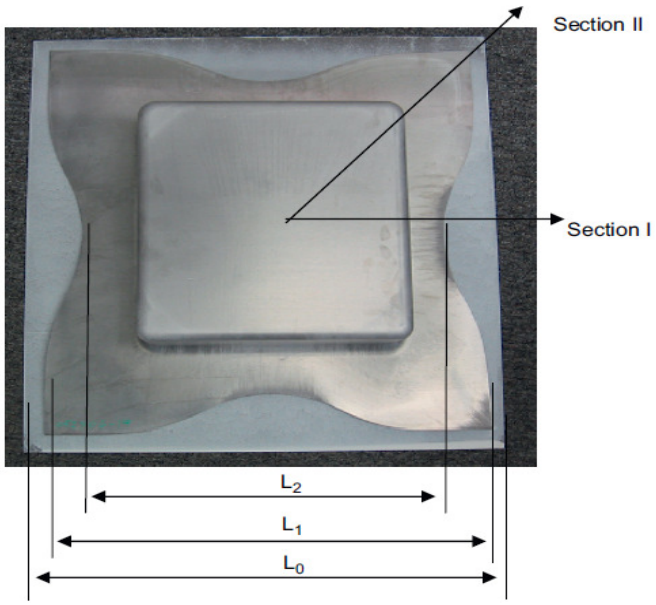

Fig. 8: Locations for measurement of material draw-in and thickness measurements [12]

Table 2: Material draw-in for experiment and simulation for SPF5083 (AA5083) [12]

Quantity	*Unit*	*Experiment*	*Simulation*
Blank holder force	kN	30	30
L0-L1	Mm	60	54
L0-L2	Mm	226	224

Note: L0 = 750 mm (Original Blank Size)

Blank thickness was measured across the final part along section I (along the plane strain section) and section II (into the corner) as noted in Fig. 8. Subsequent measurements were made every 25 mm. Figure 9 (a, b) shows the experimental and simulation results for parts formed with HDMP-SPF along sections I and II, respectively. For the gas-form only panels, failure occurred before the forming was completed therefore the corners of the panels were not finished and hence thickness data are not available for section II. Thickness data for section I are shown for the gas-formed panel in fig. 9 (a) for comparison with the thickness profiles of HDMP. Figure 9 (a, b) represented that FEA can predict the thickness distribution for the HDMP-SPF process and the HDMP-SPF

process produces a superior thickness profile to panels formed only by gas pressure. The maximum thinning at section I of parts formed with HDMP-SPF is 18% compared with that of 53% for gas-form only.

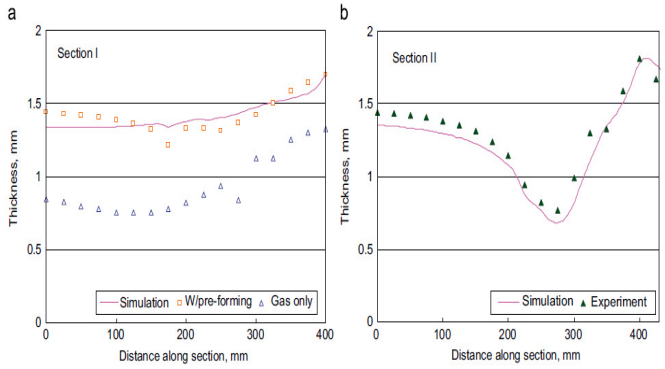

Fig. 9: Experimentally measured thickness profiles along sections (a) I and (b) II for HDMP-SPF and gas form only, and predicted thickness profiles for HDMP-SPF with SPF5083. Position from left to right represents length of line distance from the center of the part to the flange [7]

3. DESIGN AND VALIDATION OF TWO STAGE SUPERPLASTIC FORMING DIE: CASE STUDY-II

A multistage SPF approach has been applied that utilizes two stages of gas forming within one die. A schematic of two-stage gas forming is given in figure 13. During the first stage of forming, compressed air is introduced through the vent lines of the die cavity to force the sheet into an engineered preform cavity. A second gas pressure cycle is then applied through the vent lines of the preform cavity to reverse the forming direction of the sheet such that the part is formed in the opposing die cavity. The preform cavity is designed to pre-thin material in local regions of the sheet to minimize thinning and thickness distribution during the second stage forming of the die cavity.

3.1 Material & Constitutive Model

A superplastic aluminum alloy sheet, AA5083-SPF, was used in this work which had a nominal thickness of 1.22 mm. The high temperature deformation behavior of the alloy was characterized by using high temperature tensile tests. The constitutive model used for superplastic deformation was the power law equation:

$$\sigma = K \dot{\varepsilon}^{m} \varepsilon^{n} \quad (3)$$

Where, σ is effective flow stress, $\dot{\varepsilon}$ is effective strain rate, ε is effective strain, K is strength co-efficient, m is strain rate sensitivity and n is strain hardening exponent. The superplastic deformation response have been reported at 475 °C and range of strain rates between 5 x 10^{-4} and 3 x 10^{-3} s^{-1}. The chemical compositions and co-efficients are given in Table 3 and Table 4 respectively.

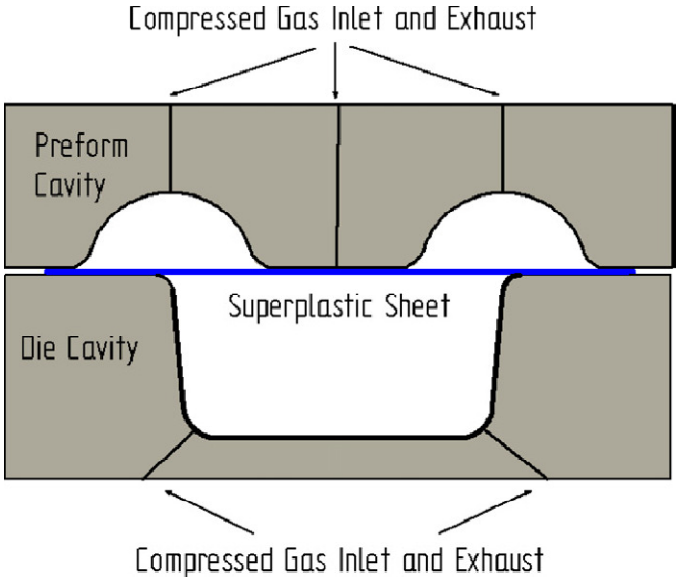

Fig. 10: Schematic illustration of two-stage superplastic forming die [5]

Table 3: Composition (wt%) of AA5083-SPF [5]

Alloy	Mg	Mn	Cr	Fe	Si	Al
AA5085	4.6	0.74	0.13	0.05	0.02	Rest

Table 4: Co-efficients for material model [5]

K	m	n
159.50	0.39	0.088

3.2 Simulation Setup

Two types of finite element analysis were used to design the preform cavity. Explicit FEA with LS-DYNA was applied in all 3-D analyses using shell elements to capture the overall thinning profile and predict wrinkles. Implicit FEA with ABAQUS was used for 2-D cross-sectional analysis with solid elements, to be capable of modeling diffuse necking after radii which is not accurately predicted with 3-D shell elements. To minimize explicit FEA simulation time, a uniform mass scaling factor of 105 was employed. The factor was determined by using sensitivity analysis of mass scaling and three baseline superplastic forming FEA models. For all 3-D models, the blank was descretized with a constant 2mm mesh element size guidelines for modeling SPF. The nodes on the perimeter of each blank were constrained to simulate the clamping of the sheet between the die halves during gas forming. The die surface was meshed with rigid triangular and quadrangular elements.

3.3 Experimental Setup

All experimental forming trials were performed with a 725 tonne superplastic forming press. Adie half was secured to each of the press platen. The platens contain cartridge heaters which heat the platen and SPF die. The die temperature was monitored using two Type K thermocouples placed within the die 25 mm from the forming cavity. Only forming trials with an average temperature of within ±3 ◦C of the target temperature of 475 ◦C were used in the post-form analysis.

The aluminum blanks were sheared to dimensions 406mm by 229mmwith the rolling direction perpendicular to the long side of the blank. Mill oil was removed from each blank with an alcohol wipe, and the blanks were coated on both sides with a proprietary SPF lubricant that contains hexagonal boron nitride. The lubricant was received in a water based suspension to permit spray-on application. It was allowed to air dry on the blanks leaving only the solid components of the lubricant on the surface. This lubricant is capable of withstanding the temperature range of aluminum SPF, provides lubricity during sheet forming and is an effective parting agent.

3.4 Two Stage SPF Die Design

The part shown in Fig. 11(a) was superplastically formed using the die shown in Fig. 11(b) and represents a portion of an automotive fender reinforcement. The outer dimensions of the die forming surface are 410mm×230mm. The entry radius of the cavity is 5mmand the maximum depth 51mm.This die can be formed with a single stage forming cycle; however, the formed panels experience a maximum thinning of 60% and a diffuse neck immediately after the entry radius. The neck was not only of structural concern but prevented the cycle time from being optimized since attempts to form the part at higher rates resulted in sheet splitting at the neck. To improve the thickness profile, a preform cavity was designed to improve the thickness profile of the part in Fig. 11(a).

3.5 FEA Driven Die Design

To design the preform surface, four cross-sections of the part cavity were generated in CAD and are shown in Fig. 12. Cross-sections 1, 2 and 3 represent the deepest portions of the cavity, as well as the location of the worst diffuse necking after the entry radius. For each cross-section, a preform was developed to strategically pre-stretch the blank and improve the thickness profile of the final part cavity triangular recesses preserves metal thickness in this region during pre-forming. This feature combined with the length of line created by the triangular pockets reduces the thinning experienced at the bottom of the part cavity.

Two-dimensional (2-D) analysis of the two-stage SPF of cross-section 2 was performed with ABAQUS. This analysis predicted the preform design to not only increase the thickness of material at the bottom of the cavity, but also prevent the formation of the diffuse necking after the entry radius. As can be seen in Fig. 17, the length of line created by the preform, changes the way metal deforms within the part cavity during the second stage of gas forming cycle.

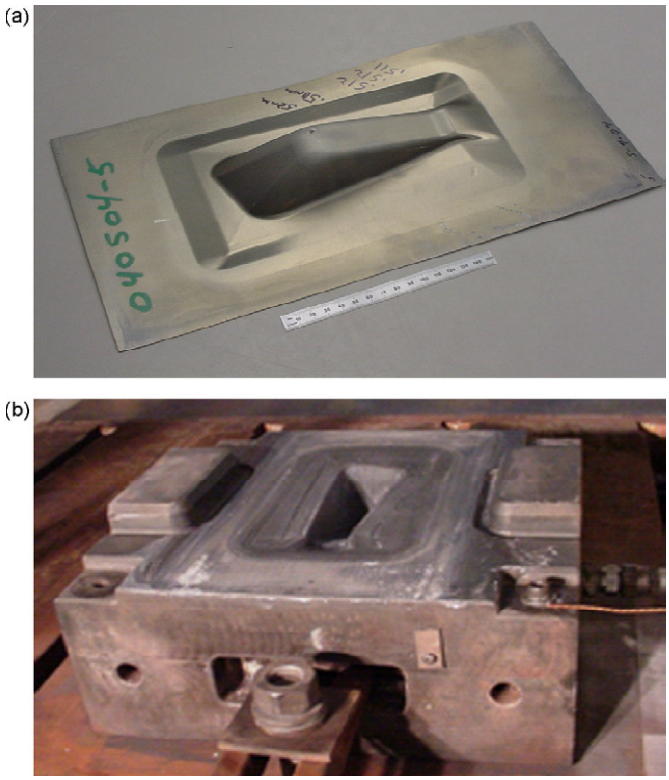

Fig. 11: The (a) part and corresponding (b) superplastic forming die cavity [5]

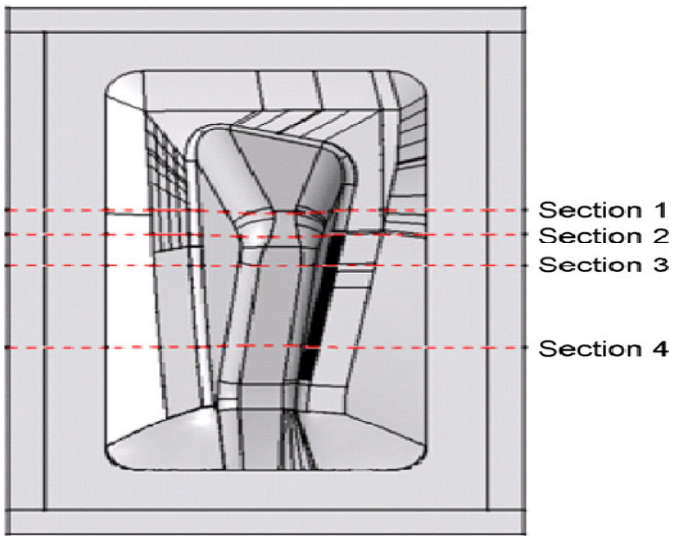

Fig. 12: Dashed lines identify the cross section of the panel for which corresponding preform cross-sections were designed [5]

Two-dimensional (2-D) analysis of the two-stage SPF of cross-section 2 was performed with ABAQUS. This analysis predicted the preform design to not only increase the thickness of material at the bottom of the cavity, but also prevent the formation of the diffuse necking after the entry radius. As can be seen in Fig. 14, the length of line created by the preform, changes the way metal deforms within the part cavity during the second stage of gas forming cycle. Compared to a single stage gas forming cycle, the stress and thinning of the sheet required to form over the entry radius during the two-stage process was significantly reduced preventing the formation of the neck.

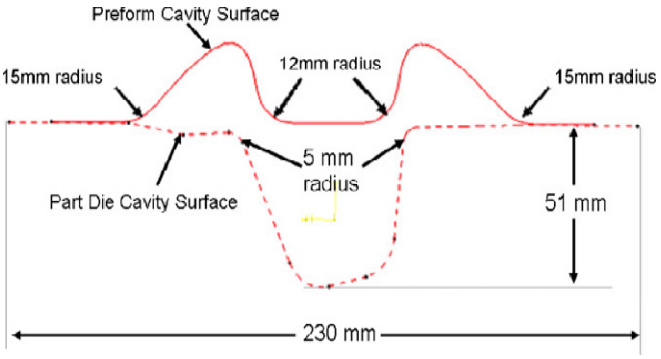

Fig. 13: Preform design (solid line) for cross-section 2 of the part cavity (dashed line) [5]

Table 5: Comparison for the length of the line for the part and corresponding preform cross sections [5]

Length of line (L)			
	Part Surface	**Preform Surface**	$L_{preform}/L_{part}$
Section 1	193	186	97%
Section 2	205	186	91%
Section 3	198	186	94%
Section 4	168	170	101%

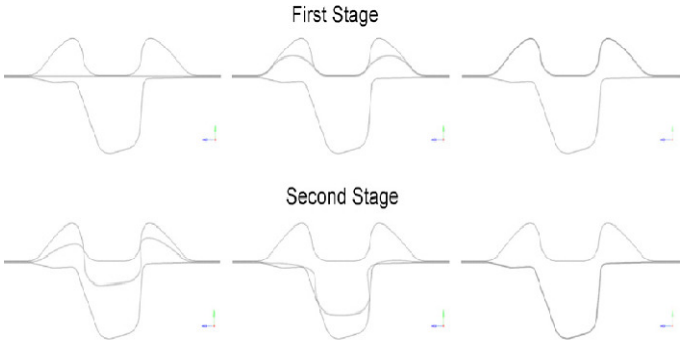

Fig. 14: 2-D FEA simulation of the two-stage forming cycle for cross-section 2 [5]

A preform cross-section was created for each of the part cross-sections in Fig. 12. The profile of the cross-sections followed the same design philosophy as described above for cross-section 2 and shown in Fig. 16. As can be seen in Table 5, the length of line for all preform cross-sections is greater than 90% of the length of line of the corresponding part cross-section. For cross-section 4, the preform length of line slightly exceeds the part cross-section length of line. Although not considered a ideal design practice for preventing wrinkles, this was done by design to provide experimental data for evaluating FEA wrinkle prediction.

The ability to predict wrinkling in SPF is essential for FEA guided die design and has not been adequately demonstrated in the literature; therefore, the wrinkles were purposely left in the design in order to gain insight into wrinkle prediction for SPF die design.

4. SUMMARY

With this present study on SPF process and case studies following observations can be drawn.

- Conventional superplastic forming has to be done with optimized process parameters. Now this will require more hit and miss approaches. To reduce the number of experiments the finite element based software can be utilized for parameters optimization.
- The explicit code LS-DYNA with power-law material constitutive equation can be used to accurately model the thinning, material draw-in and wrinkling of aluminum during HDMP-SPF.
- HDMP process achieved a forming time of 180 s as compared to over 20 min with conventional SPF.
- Material thinning was reduced in SPF5083 from a maximum of 53% to approximately 18% with the use of HDMP.
- FEA can be used to guide the design of the preform for a two stage SPF die such that the thickness profile is improved and without wrinkles.
- The necking that can develop in SPF when forming over tight radii and/or into high aspect ratio cavities can be eliminated by first preforming the sheet to redistribute metal thickness and alter the manner in which the sheet fills the cavity.
- The preform design for the two-stage process was non-intuitive and demonstrates the advantages of iterative design using finite element analysis over iterative design based on the results of experimental forming trials.
- FEA predicted thickening of the final thickness distribution should be considered to ensure wrinkles and residual defects associated with wrinkles do not develop during forming trials.

REFERENCES

[1] Al-Naib T. Y. M., Duncan J. L.,, "Superplastic Metal Forming", *International Journal of Mechanical Sciences*, 1970, pp. 463-477

[2] ASM Handbook, "Metal Working: Sheet Metal Forming", Volume 14B, *ASM International*, USA

[3] Bate P. S., Ridley N., Zhang B., Dover S., "Optimization of Superplastic Forming of Aluminum Alloy", *Journal of Material Processing Technology*, 2006, pp. 91-94

[4] Bonat J., Gil, A., Wood, R. D., Said, R., Curtis, R. V., "Simulating Superplastic Forming", *Journal of Computer Methods in Applied Mechanics and Engineering*, 2006, pp. 6580-6603

[5] George L. Jr., Friedman P., Weinmann K., "Design and Experimental Validation of Two Stage Superplastic Forming Die", *Journal of Material Processing Technology*, 2009, pp. 2152-2160

[6] Khaleel M. A., Johnson K. I., Hamilton C. H., Smith M. T., "Deformation Modeling of Superplastic AA-5083", *International Journal of Plasticity*, 1998, pp. 1133-1154

[7] Kim Y. H., Lee, J. M., Hong S. S., " Optimal Design of Superplastic Forming Processes", *Journal of Material Processing Technology*, 2001, pp. 166-173

[8] Lin J., Dunne, F. P. E., "Modeling Grain Growth Evolution and Necking in Superplastic Blow Forming", *International Journal of Mechanical Sciences*, 2001, pp. 595-609

[9] Lou T. P., Woo K. D., "Influences of Grain Size on Fracture of Superplasticity", *Journal of Materials Letters*, 2002, pp. 374-377

[10] Luckey S. G., Frieman P. A., Xia Z. C., Weinmann K. J., "Simulation of Superplastic Forming using Explicit Finite Element Analysis", *Trans NAMRI/SME*, 2006, pp. 33-37

[11] Luckey S. G., Frieman P. A., Weinmann K. J., "Correlation of Finite Element Analysis to Superplastic Forming Experiments", *Journal of Material Processing Technology*, 2007, pp. 30-37

[12] Luo Y., Luckey S. G., Friedman P. A., Peng Y., "Development of an Advanced Superplastic Forming Process Utilizing Mechanical Pre-forming Operation", *International Journal of Machine Tools & Manufacture*, 2008, pp. 1509-1518

[13] Nazzal M. A., Khraisheh M. K., Abu-Farah F. K., "The Effect of Strain Rate Sensitivity Evolution on Deformation Stability during Superplastic Forming", *Journal of Material Processing Technology*, 2007, pp. 189-192

[14] Pancholi V., Kashyap B. P., " Effect of Layered Microstructure on Superplastic Forming Property of AA8090 Al-Li Alloy", *Journal of Material Processing Technology*, 2007, pp. 214-220

[15] Raman H., Luckey S. G., Ghassan K., Friedman P. A., "Development of Accurate Constitutive Models for Simulation of Superplastic Forming, *Journal of Material Performance & Engineering*, 2007, pp. 284-292

[16] Shukla S. V., Chandrasekhrayya C., Singh R. N., Fotedar R., Sinha T. K., Kashyap B. P., "Effect of Strain Rate and Test Temperature on Superplasticity of Zr-2.5 wt% Nb Alloy", *Journal of Nuclear Materials*, 1999, pp. 130-138

[17] Wenbo H., Kaifeng Z., Guofeng W., "Superplastic Forming and Diffusion Bonding for Honeycomb Structure of Ti-6Al-4V Alloy", *Journal of Material Processing Technology*, 2007, pp. 450-454

[18] Xun Y. W., Tan M. J., "Applications of Superplastic Forming and Diffusion Bonding to Hollow Engine Blades", *Journal of Material Processing Technology*, 2000, pp. 80-85

[19] Zhang K. F., Wang G. F., Wu D. Z., Wang Z. R., "Research on controlling of thickness distribution in superplastic forming", *Journal of Material Processing Technology*, 2004, pp. 54-57